Research Article

iMedPub Journals
www.imedpub.com

Journal of Medical Physics and Applied Sciences
ISSN 2574-285X

2025
Vol.10 No.2:091

Automated Liver Surface Texture Analysis with Irregularity Index for Improved Classification of Hepatic Disorder

Huasi Hu[1*], Saadat Ali[2], Ahmer Saleem[1] and Mingfei Yan[1]

[1]Department of Nuclear Science and Technology, Xi'an Jiaotong University, Shaanxi, China

[2]Department of Nuclear Medicine and Radiotherapy, Gujranwala Institute of Nuclear Medicine and Radiotherapy, Gujranwala, Pakistan

[*]**Corresponding author:** Huasi Hu, Department of Nuclear Science and Technology, Xi'an Jiaotong University, China; E-mail: huasi_hu@mail.xjtu.edu.cn

Received date: August 10, 2024, Manuscript No. IPIMP-24-19518; **Editor assigned date:** August 13, 2024, PreQC No. IPIMP-24-19518 (PQ); **Reviewed date:** August 27, 2024, QC No. IPIMP-24-19518; **Revised date:** April 10, 2025, Manuscript No. IPIMP-24-19518 (R); **Published date:** April 17, 2025, DOI: 10.36648/2574-285X.10.2.91

Citation: Hu H, Ali S, Saleem A, Yan M (2025) Automated Liver Surface Texture Analysis with Irregularity Index for Improved Classification of Hepatic Disorder. J Med Phys Appl Sci Vol:10 No:2

Abstract

Background: The liver plays a crucial role in various physiological and pathological processes, making accurate analysis of its surface texture essential for diagnostic and therapeutic purposes. Automated methods, particularly those employing machine learning techniques have shown promise in this domain.

Purpose: To enhance the classification accuracy of liver surface texture analysis by introducing a novel feature, the irregularity index. This paper investigates the potential of this approach to provide more reliable and accurate classification results in comparison to existing methods.

Materials and methods: To achieve our research goals, we collected a dataset of liver surface textures and developed a methodology that incorporates SVM as a classification tool. We introduced the irregularity index as a new feature to capture irregularities in liver texture patterns. This feature, in combination with SVM, was employed for the automated analysis of liver surface textures.

Results: Our experimental results indicate that the inclusion of the irregularity index significantly improves the classification accuracy of liver surface textures when compared to traditional methods. The SVM-based approach, coupled with the irregularity index, achieved an impressive level of accuracy, demonstrating the potential for more precise classification of liver surface textures.

Conclusions: In conclusion, the integration of the irregularity index with support vector machine-based analysis represents a promising advancement in the field of automated liver surface texture analysis. This innovative approach has the potential to enhance the accuracy and reliability of liver disease diagnosis and prognosis., ensuring optimal radiation protection for patients, staff, and the public.

Keywords: Liver surface; Automated classification; Irregularity index; Artificial intelligence

Introduction

A biopsy constitutes a diagnostic procedure wherein a minute tissue specimen is extracted from a specific anatomical region under consideration, subsequently subjected to examination for potential irregularities [1] It is imperative to acknowledge the inherent risks associated with biopsies, as they merely represent a minuscule fraction, approximately one in fifty thousandth parts, of the entire hepatic organ. Given the diminutive size of the tissue sample obtained, it is essential to recognize that biopsy results may not consistently reflect the precise state of the entire liver, thereby yielding false negative outcomes in up to 30 percent of cases [2].

While biopsy boasts commendable accuracy, its invasive character and inherent infection risk preclude its widespread adoption as a routine diagnostic practice [3]. Consequently, a straightforward, repeatable, and cost-effective technique for diagnosing liver cirrhosis is sought after. In the context of this research endeavor, ultrasound imaging assumes a pivotal role in the diagnostic process owing to its non-invasive attributes, repeatability, and cost-effectiveness [4].

In ultrasound imaging, the identification of cirrhosis is typically characterized by specific visual cues, including irregularities in the liver surface, alterations in portal vein mean flow velocity, and an augmentation in the size of the caudate lobes [5]. Notably, the irregularity of the liver surface serves as a consistent and reliable indicator of the presence of liver cirrhosis, exhibiting a diagnostic accuracy exceeding 70 percent [6]. Additionally, the nodularity of the liver contour demonstrates a direct correlation with the presence of cirrhotic liver pathology [7]. It is worth noting that the diagnosis of cirrhosis may potentially be underestimated when relying solely on the smoothness of the liver surface as an indicator [8].

Currently, the assessment of the liver surface relies on the visual interpretation of liver images by radiologists or medical professionals. However, this manual classification approach is associated with several drawbacks. These drawbacks encompass variations in image quality attributable to disparities in imaging equipment, inherent differences between patients, and

potential data corruption, all of which pose challenges for human interpreters tasked with analyzing the liver surface [9]. Additionally, it is noteworthy that even among medical experts, there exists inter-observer variability, implying that different experts may interpret the same liver surface images differently.

To overcome these limitations, there is a growing interest in the adoption of automated or computer-assisted systems for liver surface analysis. Such systems offer a multitude of advantages, including heightened accuracy, rapid processing, reproducibility, resilience to variations in data quality, and cost-effectiveness.

Materials and Methods

Data acquisition

The ultrasound images utilized in this research were obtained using a Toshiba Aplio 500 digital ultrasound machine equipped with a convex probe, employing a specific tissue harmonic imaging frequency. The images possess dimensions of 720 × 960 × 3 pixels and are stored in bitmap format. A radiologist annotated these images, categorizing them as either displaying a smooth or irregular liver surface, and these labels serve as the reference standard for this investigation. A total of 80 ultrasound images from various subjects were acquired. The hospital ethics committee waived the approval requirement for this retrospective study, which focused on patients who had been advised to undergo liver scan by surgeons (Figure 1).

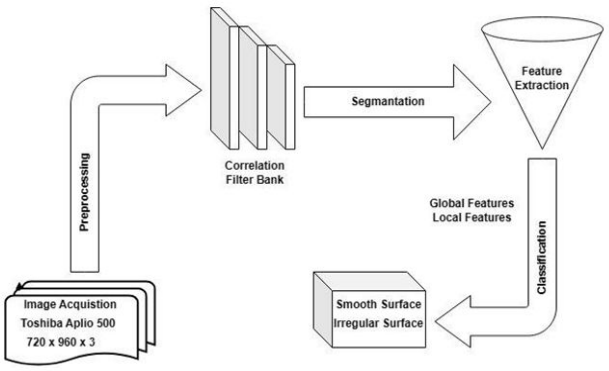

Figure 1: Complete workflow: Acquisition to classification.

To ensure consistency, the image acquisition parameters, including focus, frequency, zoom, and probe location, were maintained uniform across all images to mitigate undesirable variations.

It is worth noting that the speckle noise is an inherent characteristic of ultrasound images, adversely affecting image quality, contrast, and resolution.

Segmentation

The process of segmenting medical images is a challenging task. Specifically, the segmentation techniques frequently employed for ultrasound images encompass a spectrum of methodologies, such as thresholding, region growing, employment of classifiers, clustering techniques, utilization of Markov random field models, artificial neural networks, deformable models, as well as guided approaches.

It is clearly evident from Figure 2(d) that the Hough transform erroneously delineated the liver surface. It is observed that the correlation filter works well in segmenting or detection of horizontal liver surface parts but surface inclined to an angle is not perfectly detected (Figure 2).

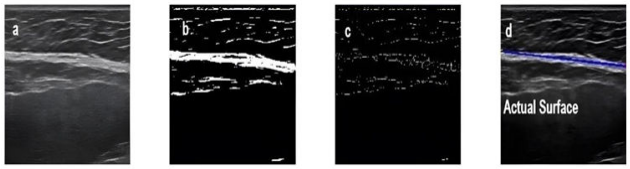

Figure 2: Hough transform segmentation.

Within the realm of image processing, Correlation Filters (CFs) represent a category of filters founded upon linear classifiers. Their primary objective is to mitigate localization errors while distinguishing between the target object and the background.

The notion of a filter bank is devised in the development of a correlation filter bank, which, in turn, contributes to the attainment of more precise segmentation.

Algorithm is developed based on Minimum Output Sum of Squared Error (MOSSE) method to produce filters by using original images and their desired images. After training on example images a robust correlation filter is generated which is then used for segmentation task. If we visually analyze filter generated (Figure 3).

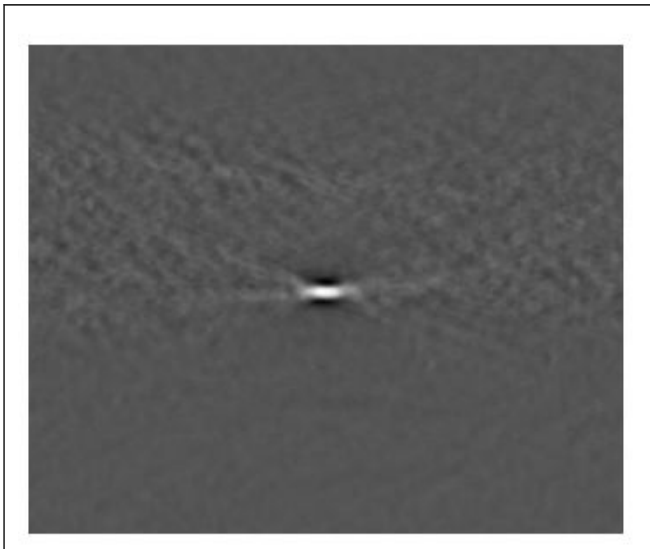

Figure 3: MOSSE correlation filter.

In ultrasound images of liver, above liver surface there is internal abdominal fat and below surface there is a dark empty region. Similarly in the filter a fat like pattern can be seen on the upper half, above the small white line, while the bottom half is empty region. This small white line in Figure 3 is actually representing liver surface in filter image. When the above filter is correlated with liver ultrasound image, similarity is found and when a pixel of higher value, whose upper portion has fat while

lower side has blank region, is found a high correlation value is assigned to that pixel in output image and vice versa.

Figure 4(b) shows the result of segmentation of original image shown in Figure 4(a). Although a small extra part of abdominal wall is also detected along with liver surface but this can be efficiently removed by post processing.

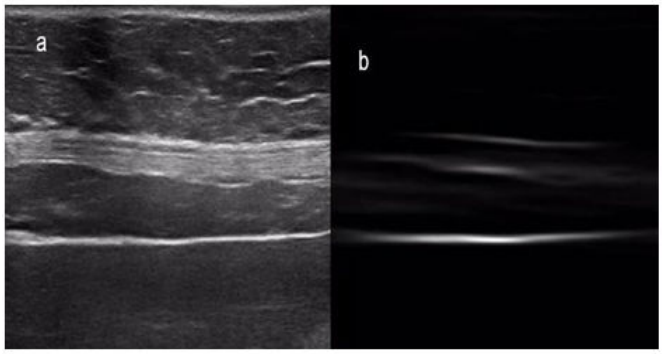

Figure 4: (a) Smooth liver surface, (b)Segmented liver surface using correlation filter.

Another result of segmentation using correlation filter for highly irregular liver surface is shown in (Figure 5)

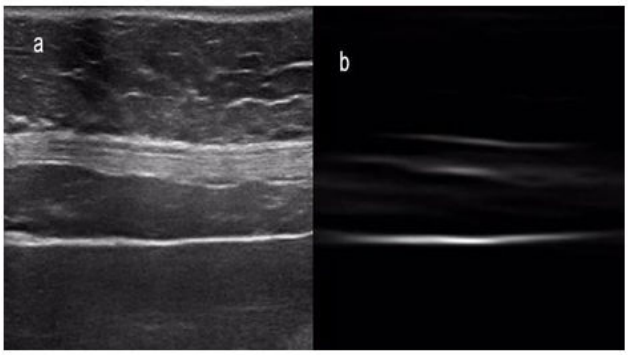

Figure 5: Highly irregular segmented surface.

It can be seen that highly accurate and clear segmentation is achieved. When convolution of image and filter is performed in Fourier domain their topological arrangement is converted into torus like shape. It is easy to understand this arrangement as left edge of the image is linked to the right edge, and the top part connected to the bottom part. In convolution the image do not translate in spatial domain instead rotated in torus plane which produces an artifact in image which is highly undesired because it affects output of correlation. This artifact reduced to minimum by applying the steps discussed by Bolme et al.

The motivation behind employing a correlation filter bank stemmed from the observation that while the correlation filter exhibited proficiency in segmenting or detecting horizontally oriented segments of the liver surface, it exhibited limitations in accurately identifying surfaces inclined at various angles. The correlation filter generated by MOSSE is used to construct filter bank. Correlation filter is rotated with an angle of 2 degree in every increment and a sequence of filters is generated. Angle range of −30 to +30 and incremental step is 2 degree is used. An array of 30 filters is generated in this way. The filter bank, in essence, comprises an array of filters that partition the input image into multiple sub-images, each of which carries a distinct output response derived from the original image. In the context of this study, the filter bank consists of an array of filters rotated at different angles. This approach enables the convolution of the filter bank with an image, yielding the desired outcomes effectively.

Subsequently, the challenges arising after the preliminary segmentation employing the filter bank are addressed through post-processing techniques.

Feature extraction

Two types of feature are extracted for liver surface analysis: Global features and local features. The features extracted from region of interest without dividing it in patches are called global features whereas local features are extracted from sub-parts of region of interest. Global features are extracted from the whole region of interest. The methods used to extract global features in this work include PCA, curve fitting and edge detection.

PCA is applied on total of 80 images. All images have same dimensions. Half of the images in dataset have smooth liver surfaces while those in other half have irregular liver surfaces. Eigen bases are computed and threshold is applied of 90% proportion of variance for dimensionality reduction using scree graph analysis. Using these Eigen bases, input images are projected to extracted principal components. PCA gives best results when different images have similar information aligned spatially. This projected data is used as features for training and testing of classifier. In our case edge detection is used for liver surface detection which is used as feature for subsequent classifier. Edge information is an important feature to classify liver surface as smooth or irregular because irregular liver surface contains more sharp changes (edges) in a defined area as compared to smooth liver surface [10-18].

The complete liver surface depicted in an image does not exhibit uniform irregularity across its entirety. Instead, irregularities manifest locally in smaller patches on the liver surface. Consequently, when employing global features for analysis, the subtle local irregularities present in the liver surface risk being overshadowed by the bulk of information pertaining to the regular surface. Therefore, the approach adopted involves the extraction and utilization of local features for the specific classification task at hand. Various local features are computed, encompassing parameters like the Irregularity Index, features derived through Principal Component Analysis (PCA), and texture-based features. To extract these local features, a window of fixed dimensions is employed, which is systematically moved across the entire image to capture local information. The choice of window size is contingent upon the size of irregularities observed in the liver surface within the dataset. Our observations reveal that the horizontal dimensions of these irregularities vary within the range of 50 to 100 pixels, with a vertical variation of approximately 25 pixels (Figure 6).

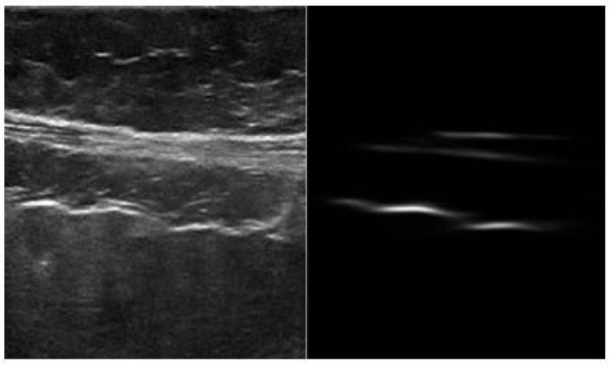

Figure 6: Window moving on liver surface.

Consequently, a window with dimensions of 100 × 50 pixels is selected. Additionally, to ensure that these windows effectively capture the smallest horizontal irregularity dimension, a step size of 50 pixels is employed, facilitating the extraction of subsequent windows, as illustrated in (Figure 6).

In local feature extraction, PCA is applied on windows extracted from liver surface. Liver surfaces in all windows are rotated to such an angle that surfaces become horizontal. In this way all windows have aligned liver surfaces. After alignment, contrast adjustment and normalization is applied on windows. These aligned, normalized and contrast adjusted windows are introduced to PCA for feature extraction.

A new feature named as irregularity index is developed for liver surface classification task. It is computed by taking absolute difference between thinned liver surface and a line fitted to points of this surface in local window. This feature shows the deviation of liver surface from a regular line. More the deviation, higher the value of irregularity index. These features have shown best classification results among all the features extracted in this work. The concept of irregularity index is shown in (Figure 7). A thinned liver surface is shown and two windows checking the irregularity are shown on top. In left window, the liver surface and the fitted line has very small deviation from each other while in right window irregularity is there because the deviation between fitted line and liver surface line is high.

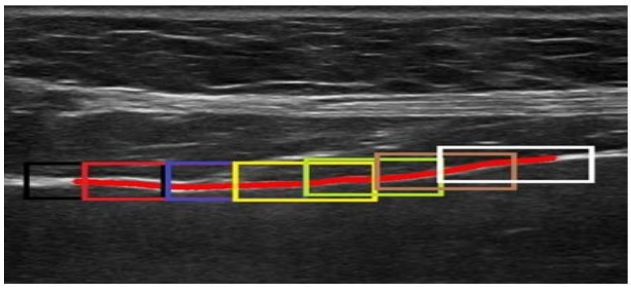

Figure 7: Shows original MATLAB images of windows, in which liver surface is shown by white line while the fitted line in red.

It can be clearly seen in (Figure 8) that there is very small overlap of values between two classes using these features. Smooth surface class has low values of irregularity index while irregular surface class has higher values of irregularity index.

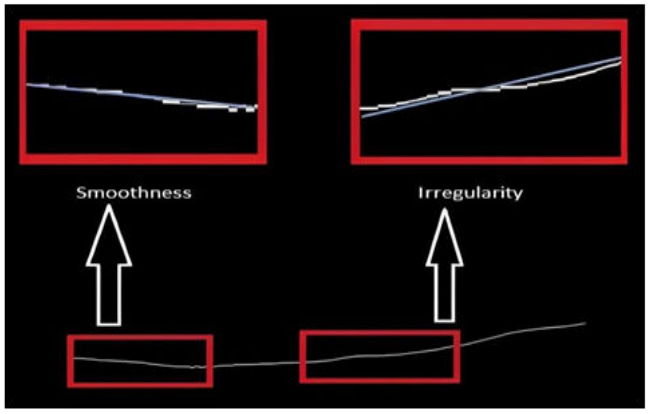

Figure 8: Box plot between irregular and smooth surface classes on basis of irregularity index as feature.

High classification accuracy has been achieved using irregularity index based features as compared to other features extracted. PCA is also applied on local information extracted from liver surface but it has shown moderate classification accuracy

Classification

We implement the "leave one image out" cross-validation technique. In this classification process, the label assigned to the class representing irregular liver surfaces is denoted as +1, while the label for smooth liver surfaces is represented as -1.

Results

The examination reveals that the irregularity Index stands out as the most effective feature for the classification task at hand with AUROC of 0.94 for irregularity index. The feature extraction methods were based on global and local features. The global features include PCA and edge based with AUROC of 0.75 and 0.74 respectively. Whereas, local features include texture, PCA and Irregularity index with AUROC of 0.78,0.74 and 0.94 respectively. Various combinations of different features were experimented with in an effort to assess whether such combinations could enhance classification accuracy. As a result, the ultimate decision was to adopt the Irregularity Index as the final and most suitable approach. The results are tabulated in Table 1.

Table 1: AUROC for different features.

Extraction Method	Global	Local

Features	PCA	Edge based	Irregularity Index	PCA	Texture
AUROC	0.75	0.74	0.94	0.7494	0.78

Discussion

The assessment criterion utilized throughout this study was the Area under the Receiver Operating Characteristic (ROC) curve. Initially, for features derived from PCA, three distinct strategies were explored. These strategies encompassed PCA applied to Regions of Interest (ROIs) without global surface alignment, PCA applied to ROIs with global surface alignment, and PCA applied to ROIs with local surface alignment.

The initial investigation involved the application of PCA to ROIs without aligning surfaces globally, wherein a classification task involving 80 individuals was conducted using the leave-one-person-out cross-validation technique. Subsequently, an ROC curve was plotted to evaluate classification accuracy. The outcome revealed an Area under the Curve (AUC) of 0.60, indicating that this particular approach was inadequate for our specific task. In a similar vein, when the classification was based on PCA features extracted from ROIs with globally aligned liver surfaces, the AUC was found to be 0.70. This result demonstrated an improvement in classification accuracy when employing features extracted via PCA in conjunction with aligned liver surfaces.

Furthermore, in the context of local feature extraction, features based on PCA were extracted from a total of 519 windows obtained from 80 images, and these windows were assigned labels corresponding to their parent images. Contrary to the initial expectation of achieving a higher Area under the Receiver Operating Characteristic (AUROC) score using this particular feature, the results did not meet the anticipated performance levels.

Subsequently, features based on edges, extracted globally, were employed for classification purposes. An evaluation involving 80 images was conducted, utilizing the leave-one-out cross- validation technique with these features. A resulting ROC curve was generated, and the corresponding AUROC was found to be 0.74, indicating a moderate level of classification performance. Classification results based on texture features yielded an AUROC of 0.78 as shown in Figure 9.

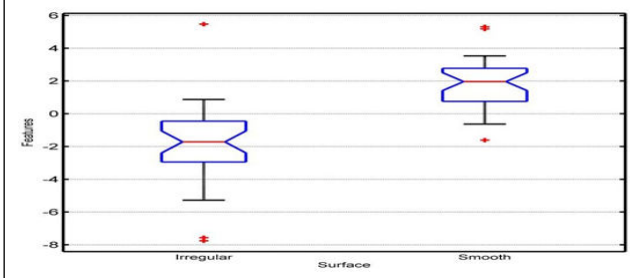

Figure 9: ROC curve for classification based on texture features.

Finally, features based on the Irregularity Index were employed with a local feature extraction approach. For classification purposes, various statistical operations were applied to this array, encompassing mean, minimum, maximum, and standard deviation. ROC curves were generated based on these classifications, and the maximum area under the curve (0.9231) was achieved when utilizing the mean value of the irregularity index as evident from (Figure 10). Furthermore, when a combination of the maximum, minimum, and mean values of the Irregularity Index was employed for classification through the leave-one-person-out cross-validation method, an AUROC of 0.94 was attained.

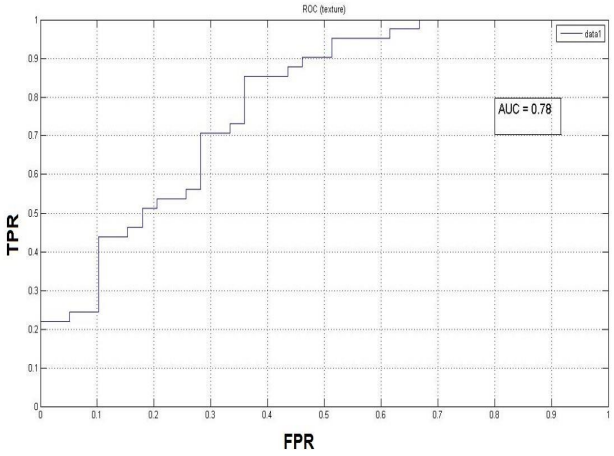

Figure 10: ROC Curve for classification based on different statistical interpretation of irregularity index as feature.

Conclusion

In Conclusion, the most challenging aspect of this research endeavor resides in the segmentation of liver images. Segmentation tasks within the realm of medical imaging are inherently complex, and in this particular instance, the resemblance between the abdominal wall and the liver surface further compounds the intricacy of the segmentation process. Numerous techniques were employed in an attempt to achieve an accurate liver surface segmentation, ultimately culminating in the utilization of a correlation filter, which proved to be aptly suited for this demanding task.

The second fundamental objective revolves around feature selection, wherein diverse features such as PCA, texture-based, and edge-based features were extracted. Regrettably, these features failed to yield satisfactory classification results. To address this limitation, a local feature extraction technique was developed; introducing a novel feature termed the "irregularity index. Notably, the Area under the Receiver Operating

Characteristic (AUROC) achieved based solely on the irregularity index, without the use of any classifier, reached a remarkable value of 0.94, underscoring the efficacy of this feature.

References

1. Phipps WS, Kilgore MR, Kennedy JJ, Whiteaker JR, Hoofnagle AN, et al. (2023) Clinical proteomics for solid organ tissues. Mol Cell Proteomics 22(11):100648
2. Chowdhury AB, Mehta KJ (2023) Liver biopsy for assessment of chronic liver diseases: a synopsis. Clin Exp Med 23:273-285
3. Guglielmo FF, Barr RG, Yokoo T, Ferraioli G, Lee JT, et al. (2023) Liver fibrosis, fat, and iron evaluation with MRI and fibrosis and fat evaluation with US: a practical guide for radiologists. Radiographics 43:e220181
4. Jung, EM (2023) Current aspects of multimodal ultrasound liver diagnostics using contrast-enhanced ultrasonography (CEUS), fat evaluation, fibrosis assessment, and perfusion analysis–An update. Clin Hemorheol Microcirc 83:181-193
5. Nepal P, Crowley C, Harisinghani M (2023) Conventional liver imaging in hepatitis. In: Comprehensive Guide to Hepatitis Advances. 1 ed.: Academic Press 61-86
6. Maheshwari S, Gu CN, Caserta MP (2023) Imaging of Alcohol-Associated Liver Disease. AJR 1:1-15
7. Sarfati E, Bone A, Rohe MM, Gori P, Bloch I (2023) Learning to Diagnose Cirrhosis from Radiological and Histological Labels with Joint Self and Weakly-Supervised Pretraining Strategies. 1-4
8. Ramamoorthy S, Sivasubramaniam R (2018) Image Processing Including Medical Liver Imaging: Medical Image Processing from Big Data Perspective, Ultrasound Liver Images, Challenges. 380-392
9. Sun Y, Zhao Y, Sun J (2020) Subjective Image Quality Assessment: A Pre-Assessment on Visual Distortion of Medical Images by Clinicians and Radiologists. ICISCE 1367-1370
10. Popa SL, Ismaiel A, Abenavoli L, Padureanu AM, Dita MO, et al. (2023) Diagnosis of liver fibrosis using artificial intelligence: a systematic review. Medicina 59:992
11. Liu J, Li C, Liu L (2023) Speckle noise reduction for medical ultrasound images based on cycle-consistent generative adversarial network. 86:1023-1036
12. Luijten B, Chennakeshava N, Eldar YC (2023) Ultrasound signal processing: from models to deep learning. Ultrasound Med Biol 49:677-698
13. Zhang J, Feng W, Yuan T (2022) SCSTCF: spatial-channel selection and temporal regularized correlation filters for visual tracking. Applied Intelligence 53:7697-7712
14. He J, Ji Y, Sun X, Wu S, Wu C, et al. (2023) Learning Background-Suppressed Dual-Regression Correlation Filters for Visual Tracking. Sensors 23:5972-5992
15. Andre G (2005) Separable linear classifiers for online learning in appearance-based object detection. 3691:347-354
16. Bolme, David S, Bruce A (2009) Average of Synthetic Exact Filters. 2105-2112
17. Haggag S (2022) A Computer-Aided Diagnostic System for Diabetic Retinopathy Based on Local and Global Extracted Features. Appl Sci 12:8326-8340
18. Vasundhara N, Nandan AS, Hemanth SV (2023) An Efficient Biomedical Solicitation in Liver Cancer Classification by Deep Learning Approach. 01-05